Journal of Neuroscience Methods 320 (2019) 128–137

Contents lists available at ScienceDirect

Journal of Neuroscience Methods

journal homepage: www.elsevier.com/locate/jneumeth

Evaluating the applicability of mouse SINEs as an alternative normalization approach for RT-qPCR in brain tissue of the APP23 model for Alzheimer's disease

Jana Janssens[a,1], René A.J. Crans[b,c,1], Kathleen Van Craenenbroeck[b], Jo Vandesompele[d,e], Christophe P. Stove[b], Debby Van Dam[a,f,*], Peter P. De Deyn[a,f,g,h]

[a] Laboratory of Neurochemistry and Behavior, Institute Born-Bunge, University of Antwerp, Universiteitsplein 1, BE-2610 Wilrijk, Belgium
[b] Laboratory for GPCR Expression and Signal Transduction (L-GEST), Laboratory of Toxicology, Ghent University, Ottergemsesteenweg 460, BE-9000 Ghent, Belgium
[c] Unitat de Farmacologia, Departament Patologia i Terapèutica Experimental, Facultat de Medicina, IDIBELL, Universitat de Barcelona, 08907 L'Hospitalet de Llobregat, Spain
[d] Center for Medical Genetics, Ghent University Hospital, C. Heymanslaan 10, BE-9000 Ghent, Belgium
[e] Cancer Research Institute Ghent (CRIG), Ghent University, BE-9000 Ghent, Belgium
[f] Department of Neurology and Alzheimer Center, University Medical Center Groningen (UMCG), Hanzeplein 1, 9713 GZ Groningen, the Netherlands
[g] Department of Neurology and Memory Clinic, Hospital Network Antwerp (ZNA) Middelheim and Hoge Beuken, Lindendreef 1, BE-2020 Antwerp, Belgium
[h] Biobank, Institute Born-Bunge, University of Antwerp, Universiteitsplein 1, BE-2610 Antwerp, Belgium

ARTICLE INFO

Keywords:
Reference genes
B elements
APP
C57BL/6J

ABSTRACT

Background: The choice of appropriate reference genes (RGs) for use in reverse transcription quantitative polymerase chain reaction (RT-qPCR) has been thoroughly investigated, since the inclusion of unstable RGs might cause inaccurate gene expression results.

New method: Short interspersed nuclear elements (SINEs) such as B elements, might represent an alternative solution given the high occurrence of these repetitive elements in the rodent genome and transcriptome. We performed RT-qPCR to investigate the stability of nine commonly used RGs and two B elements, B1 and B2, across different age- and genotype-related experimental conditions in the hippocampus and cortex of the APP23 amyloidosis mouse model for Alzheimer's disease. Gene stability was assessed using geNorm, NormFinder and BestKeeper. Human amyloid precursor protein (*APP*) levels in transgenic versus wild-type animals were also determined to validate the use of B elements as an alternative normalization approach.

Results: Whereas B elements were stably expressed in the hippocampus, they were ranked as least stable in the cortex. The optimal normalization factor (NF) in hippocampus was a combination of *Gapdh* and *Rpl13a*, whereas in cortex, *Actb* and *Tbp* constituted the ideal NF.

Comparison with existing method: When comparing B1 and B2 as NFs for *APP* with the optimal panel of RGs in hippocampus, we found that B1 and B2 performed similarly to the optimal NF, while these SINEs performed less well in cortex.

Conclusions: Although B elements are suitable as an alternative normalization strategy in the hippocampus, they do not represent a universal normalization approach in the APP23 model.

1. Introduction

The reverse transcription quantitative polymerase chain reaction (RT-qPCR) is one of the most commonly used techniques in the field of molecular biology (de Jonge et al., 2007), and has become the gold standard for quantification of mRNA in biological samples (Bustin,

Abbreviations: APP, amyloid precursor protein; Aβ, amyloid beta; geNorm M, average expression stability; geNorm V, pairwise variation between normalization factors incorporating a consecutive number of reference genes; HET, heterozygous; NF, normalization factor; NRQ, normalized relative quantities; RG, reference gene; RT-qPCR, reverse transcription quantitative polymerase chain reaction; SD, standard deviation; SINE, short interspersed nuclear element; WT, wild-type

* Corresponding author at: Laboratory of Neurochemistry and Behavior, Institute Born-Bunge, University of Antwerp, Campus Drie Eiken, Universiteitsplein 1, BE-2610 Wilrijk, Belgium.
E-mail addresses: d.c.j.van.dam@umcg.nl, debby.vandam@uantwerpen.be (D. Van Dam).
[1] These authors contributed equally to this work.

https://doi.org/10.1016/j.jneumeth.2019.03.005
Received 5 December 2018; Received in revised form 27 February 2019; Accepted 4 March 2019
Available online 05 March 2019

2000; Bustin et al., 2005) given its flexibility, sensitivity, specificity and the possibility for high-throughput analyses. Quantitative determination of gene expression is either relative or absolute, however, both methods are associated with a number of pitfalls. Since absolute quantification requires the inclusion of a standard curve (Bustin, 2000; Fronhoffs et al., 2002; Pfaffl and Hageleit, 2001), a major downside of this method is the need for such a serial dilution on each plate, thus hampering large RT-qPCR studies incorporating many samples and/or genes. In contrast, the delta-delta Cq method (Livak and Schmittgen, 2001) for relative quantification normalizes expression of the gene of interest to one or more endogenous reference genes (RGs), serving as internal controls. The internal control genes should ideally be constitutively and stably expressed across cell/tissue types, developmental stages, age and treatment conditions.

The selection and validation of appropriate RGs received a lot of attention in the previous decade (De Spiegelaere et al., 2015; Guénin et al., 2009; Rydbirk et al., 2016; Svingen et al., 2015), as the inclusion of unstably expressed RGs might give rise to an important source of bias. As such, commonly used RGs including glyceraldehyde-3-phosphate dehydrogenase (*GAPDH*), beta-actin (*ACTB*), and 18S rRNA have repeatedly been shown to be variably expressed across experimental parameters and tissues (de Jonge et al., 2007; Eissa et al., 2016; Svingen et al., 2015). Another topic of discussion was the ideal number of RGs to be included in the experimental design. Following the publication of the MIQE (Minimum Information for Publication of Quantitative Real-Time PCR Experiments) guidelines for studies reporting RT-qPCR results, which recommended the inclusion of at least two RGs (Bustin et al., 2009), a restricted literature review investigated the number of RGs used in gene expression studies in the period from 2010 until 2015, showing that merely 13% of all gene expression studies used more than one RG (Chapman and Waldenström, 2015). Another survey investigating papers published from 2009 until 2011 in journals with a wide range of impact factors (IF), noted that almost 30% of journals with an IF < 5 and 73% of high-impact journals failed to publish a single paper including validated RGs (Bustin et al., 2013). The notion that (the number of) appropriate RGs should be validated for each experimental design, is currently becoming increasingly accepted in the field. However, the repeated validation of RGs for each new study entails important disadvantages, as it renders genetic research more expensive and labor-intensive. Limited RNA sample availability also hinders an extensive investigation of appropriate RGs. These drawbacks, in addition to the unstable expression of historical RGs (e.g. *GAPDH*, *ACTB* and 18S rRNA), motivate the search for alternative normalization approaches. Short interspersed nuclear elements (SINEs) are a class of highly occurring retrotransposons, which are generally 100–500 base pairs (bp) in length (Ichiyanagi, 2013; Singer, 1982). Since SINEs make up approximately 10% of the total mammalian genome (Bovine Genome Sequencing Analysis Consortium et al., 2009; Mouse Genome Sequencing Consortium et al., 2002; Lander et al., 2001; Lindblad-Toh et al., 2005; Mikkelsen et al., 2007) and since they are mainly located in intronic and untranslated regions of many genes (Tsirigos and Rigoutsos, 2009), it is hypothesized that temporary or event-related changes in a certain number of genes will not have a large impact on the overall SINE content in the transcriptome (Renard et al., 2018; Crans et al., 2019). Therefore, SINEs might represent a valuable alternative to the regularly used RGs. As an example, expressed Alu repeats were previously found to be an accurate normalization tool for RT-qPCR studies in human blood (Marullo et al., 2010), human embryonic stem cells (Vossaert et al., 2013), and cancer cells (Rihani et al., 2013). This family of retrotransposons, derived from 7SL RNA (Ullu and Tschudi, 1984; Weiner, 1980), is ubiquitously present in the primate genome (Deininger, 2011), and contains a common restriction site for AluI (Houck et al., 1979). Due to the ability to integrate in various regions of the genome, Alu repeats can regulate gene expression by acting as transcriptional enhancers (Sasaki et al., 2008), by influencing pre-mRNA splicing (Lev-Maor et al., 2003; Sorek et al., 2002) or other documented mechanisms (for review, see Brosius, 1999; Elbarbary et al., 2016; Tomilin, 1999).

The identification of a second family of SINEs, present in the rodent genome (Kramerov et al., 1979; Krayev et al., 1980, 1982), arose from the analysis of the structural features of pre-mRNA (Ryskov et al., 1972). Its nomenclature is based on the homology to double-stranded (ds) regions in pre-mRNA, termed as dsRNA-B molecules (Kramerov et al., 1979; Ryskov et al., 1972, 1973). Further analysis of the DNA sequences complementary to dsRNA-B showed two abundant categories, B1 and B2 (Kramerov et al., 1979), each with a distinct degree of sequence variation (Kramerov et al., 1979), and derived from distinct RNA ancestor molecules. The first category, B1, consists of sequences with a total length of 130 bp (Krayev et al., 1980). Similar to Alu repeats, B1 elements are derived from 7SL RNA and were termed quasi-dimers because of an internal duplication of 29 bp (Labuda et al., 1991; Veniaminova et al., 2007). In contrast, B2 sequences, which are generally 190 bp in length, originate from tRNA (Daniels and Deininger, 1985; Sakamoto and Okada, 1985). Analogous to the Alu repeats, B elements are hypothesized to be involved in splicing, processing of RNA polymerase II transcripts, and the regulation of gene expression (Krayev et al., 1982). Thus, since B1 and B2 elements are well characterized and because of their ubiquitous presence in the rodent genome and transcriptome, these SINEs might represent an interesting alternative to classical RGs in RT-qPCR experiments. In this paper, we investigated the applicability of nine commonly used mouse RGs: *Gapdh*, *Actb*, beta-2-microglobulin (*B2m*), phosphoglycerate kinase 1 (*Pgk1*), hypoxanthine guanine phosphoribosyl transferase (*Hprt*), tyrosine 3-monooxygenase/tryptophan 5-monooxygenase activation protein zeta (*Ywhaz*), beta-glucuronidase (*Gusb*), TATA-box binding protein (*Tbp*) and ribosomal protein L13a (*Rpl13a*), as well as B1 and B2 elements as a normalization strategy for gene expression analysis in hippocampal and cortical tissue of the APP23 amyloidosis mouse model for Alzheimer's disease (AD). Although various work reported about methylation of B elements (Tommasi et al., 2013), posttranscriptional gene regulation (Lucas et al., 2018), and their transcriptional response to viral cell infection (Williams et al., 2004), few previous studies used these SINEs as a normalization approach for RT-qPCR experiments. Only one recent study performed a similar experimental analysis concerning the applicability of B elements for normalization of gene expression in hippocampus and cortex of a rat model of temporal lobe epilepsy (Crans et al., 2019), while, to the best of our knowledge, these SINEs have not previously been used for analogous purposes in mice.

2. Materials & methods

2.1. Animal model and tissue collection

The APP23 model is a transgenic mouse model, containing human cDNA of amyloid precursor protein gene (*APP*) with the Swedish double mutation (K670N/M671L), resulting in overexpression of *APP* and causing a familial form of early-onset AD in humans. From the age of 6 months onwards, APP23 mice display neuropathological lesions, i.e. Aβ plaques and tau-related pathology (Sturchler-Pierrat et al., 1997; Sturchler-Pierrat and Staufenbiel, 2000; Van Dam and De Deyn, 2011). Further characterization with respect to cognitive and behavioral abnormalities, and validation of this model, have been described previously (Van Dam and De Deyn, 2011; Van Dam et al., 2005). Male mice were group-housed in standard mouse cages in the animal facility of the University of Antwerp, in a 12:12 h light-dark cycle (lights on at 8:00 AM, lights off at 8:00 PM). Room temperature was maintained constant at 22 ± 2 °C, while the humidity was 55 ± 5%. Food and water were supplied ad libitum. Genotyping was performed on tissue derived from ear punches using custom primers (Biolegio, Nijmegen, The Netherlands). Heterozygous (HET) (n = 5) and wild-type (WT) (n = 5) mice belonging to each age group (6–8 weeks, 6, and 24 months) were euthanized by cervical dislocation, followed by brain collection and

regional dissection of each hemisphere using binoculars. First, both bulbi were dissected, followed by the cerebellum and pons/brain stem. Cortex tissue was sliced off using a scalpel, and as such removed from the underlying white matter. In addition, cortical tissue was visually checked for remaining pieces of white matter. A small sagittal midline incision was made to detach the left and right hippocampus from the fornix, after which a forceps was used to remove both hippocampi in the caudolateral direction. Tissue samples were immediately snap-frozen in liquid nitrogen and stored at −80 °C until further use. All procedures involving animals were approved by the local ethics committee for laboratory animal experiments (file number 2016-06) and complied with the European Communities Council Directive (2010/63/EU) and ARRIVE guidelines.

2.2. RNA extraction and cDNA synthesis

All analyses were performed on left hemispheric cortices (n = 30) and hippocampi (n = 29), derived from HET and WT animals aged 6–8 weeks, 6 and 24 months, except for one right hemispheric hippocampus implemented in the 24-month-old group. RNA extraction was performed using the RNeasy® Plus Universal Mini kit (Qiagen, Hilden, Germany) following the manufacturer's instructions. In addition, on-column DNase treatment was performed using the RNase-free DNase set (Qiagen, Hilden, Germany) according to the manufacturer's instructions. RNA eluate volume varied between 22 and 25 µl. RNA concentration and purity were determined by UV-VIS spectroscopy measurements at 230, 260 and 280 nm with the Nanodrop 1000 instrument (ThermoFisher Scientific, Waltham, MA, USA). Individual tissue weights, RNA yield and purity are comprised in Table A.1 (Appendix A). Reverse transcription was performed on 800 ng RNA, using the iScript cDNA Synthesis kit (Bio-Rad Laboratories, Hercules, CA, USA) in 20 µL reactions. To analyze expression stability of B elements and *Hprt* in hippocampus, cDNA samples were diluted 1:1000, while a dilution of 1:10 was adopted for *Actb*, *B2m*, *Gapdh*, *Gusb*, *Pgk1*, *Tbp*, *Rpl13a* and *Ywhaz*. In addition, cDNA was diluted 1:10 for *Actb*, *B2m*, *Gusb*, *Hprt*, *Pgk1*, *Tbp*, *Rpl13a* and *Ywhaz*, and 1:1000 for *Gapdh* and B elements in the case of cortical samples. Expression levels of the human *APP* construct as well as mouse *App* were also analyzed, and normalized to the best combination of RGs according to gene stability software, or to B elements. For this analysis, cDNA was diluted 1:10 and 1:1000 for hippocampus and cortex, respectively. All cDNA samples were stored at −80 °C until further use.

2.3. Primer design

Primers for all RGs were developed and checked for specificity using the NCBI Primer-BLAST software (Table 1) and RefSeq mRNA sequences of *Mus musculus*, while sequences for B1 and B2 elements were designed using Primer3 software, and checked for specificity using NCBI Primer-BLAST (J.V., UGent). All primers were synthesized by Biolegio (Nijmegen, The Netherlands).

2.4. Reverse transcription quantitative PCR

Reverse transcription quantitative PCR analyses were performed on the Applied Biosystems StepOnePlus instrument (Foster City, CA, USA), with automatic threshold settings. All analyses were carried out in 10 µL reactions containing 5 µL of the Power SYBR Green Master Mix (Applied Biosystems, Foster City, CA, USA), 1.5 µL of each primer (250 nM final concentration) and 2 µL cDNA (8 ng and 0.08 ng cDNA in case of a 1:10 dilution and 1:1000 dilution, respectively). Cycling conditions for all analyses consisted of initial denaturation at 95 °C during 10 min, followed by 40 cycles of denaturation at 95 °C for 15 s and annealing at 60 °C for 60 s. Finally, melting curve analysis was performed by heating from 60 °C to 95 °C in increments of 0.3 °C/s. cDNA samples and corresponding negative control reactions to which no reverse transcriptase was added during cDNA synthesis (-RT reactions), were analyzed in triplicate using StepOne Software v2.3 (Applied Biosystems, Foster City, CA, USA). All corresponding -RT reactions were negative (defined as reactions with an undetermined Cq or if the difference between the -RT control and the corresponding cDNA sample was ≥ 10 Cq values). PCR efficiencies for each assay were determined using technical triplicates of 1:2 or 1:10 serial dilutions, consisting of up to six dilution points, of a representative cDNA sample and are displayed in Table 1. Normalized relative quantities (NRQs) of B elements and *APP* were calculated using the qbase+ software (version 3.1, Biogazelle), implementing an efficiency-corrected delta-delta Cq method (Hellemans et al., 2007). Melt curves of each RT-qPCR product are shown in Appendix A.

2.5. Software and statistical analysis

Gene stability analysis was carried out on previously mentioned nine RGs, in conjunction with the two B elements separately and combined. We analyzed all RGs using qbase+ software, version 3.1, incorporating the geNorm algorithm (Vandesompele et al., 2002). This algorithm ranks distinct RGs based on the geNorm M value, which represents the average pairwise variation of remaining RGs after stepwise exclusion of the least stable genes. In addition, the geNorm V value indicates the pairwise variation of two sequential NFs upon inclusion of additional genes. Respective cutoff values for geNorm M and V are 0.50 and 0.15, so that all RGs with a geNorm M value < 0.50 are generally classified as stable RGs. A geNorm V value < 0.15 indicates that there is no benefit in including additional RGs for normalization purposes. Moreover, the NormFinder algorithm, v0.953, was used as an add-on in Microsoft Excel and ranks RGs taking into account a systematic error measure based on the inter- and intragroup variation. Similar to geNorm, the RG with the lowest stability value, is ranked as most stable (Andersen et al., 2004). Raw Cq values were transformed into efficiency-adjusted relative quantities before performing the NormFinder analysis, as described previously (De Spiegelaere et al., 2015). Lastly, the BestKeeper algorithm, version 1, was implemented in Microsoft Excel, calculating the geometric mean of all RGs included in the study as the BestKeeper Index, as well as the correlation coefficient of each individual gene with aforementioned index. Consequently, the gene with the highest correlation factor, is characterized by the most stable expression.

Since these three algorithms use distinct approaches to rank RGs, we compared the stability scores from geNorm, NormFinder and BestKeeper, and finally, compiled them into one final rank using the RankAggreg package (Pihur et al., 2009) in R, version 3.4.0 for Windows, using the cross-entropy Monte Carlo algorithm with Spearman's footrule distance (File A.1 in Appendix A).

Relative quantities of B elements and *APP*, either normalized to the optimal NF as determined by rank aggregation analysis, or to a NF containing B elements in the case of *APP*, were log-transformed for all statistical analyses. Test statistics were considered statistically significant if $P < 0.05$. To detect the effects of age and genotype on NRQs of *APP* and B elements, two-way ANOVA was applied, with Tukey's post-hoc tests for age, if applicable. In case the assumption of equality of variances was violated, separate one-way Welch's ANOVA and independent samples t-tests were performed. All statistical analyses were performed in IBM SPSS Statistics for Windows, version 24.0.

3. Results

3.1. Sample size

In total, 30 mice were included in the RT-qPCR experiments. Age groups of 6–8 weeks, 6, and 24 months, consisted of 10 mice each, with 5 HET APP23 animals and 5 WT littermates in all age groups.

Table 1
Primer sequences, amplicon lengths and PCR efficiencies of every assay. Abbreviations: *Actb*: beta-actin; *B2m*: beta-2-microglobulin; bp: base pairs; *Gapdh*: glyceraldehyde-3-phopshate dehydrogenase; *Gusb*: beta-glucuronidase; *Hprt*: hypoxanthine guanine phosphoribosyl transferase; *Pgk1*: phosphoglycerate kinase 1; *Rpl13a*: ribosomal protein L13 A; *Tbp*: TATA-box binding protein; *Ywhaz*: tyrosine 3-monooxygenase/tryptophan 5-monooxygenase activation protein zeta.

Symbol	Sequence	Accession number	Amplicon length (bp)	PCR efficiency (%)
Actb	5'-GGCTGTATTCCCCTCCATCG-3' 5'-CCAGTTGGTAACAATGCCATGT-3'	NM_007393.5	154	97.3
APP	5'-AGAAGGACAGACAGCACACC-3' 5'-TCATAACCTGGGACCGGATCT-3'	NM_001136130.2	90	94.5
B1 element	5'-GTGGCGCACGCCTTTAAT-3' 5'-GCTGGCCTCGAACTCAGAAA-3'	NC_000067.6	68	95.3
B2 element	5'-CAATTCCCAGCAACCACATG-3' 5'-ACACACCAGAAGAGGGCATCA-3'	NC_000067.6	69	98.8
B2m	5'-GTATACTCACGCCACCCACC-3' 5'-TGGGGGTGAATTCAGTGTGAG-3'	NM_009735.3	193	108.6
Gapdh	5'-AGGTCGGTGTGAACGGATTTG-3' 5'-GGGGTCGTTGATGGCAACA-3'	NM_001289726.1	95	98.5
Gusb	5'-GGCGATGGACCCAAGATACC-3' 5'-TGAATCCCATTCACCCACACA-3'	NM_010368.1	88	106.0
Hprt	5'-CTTCCTCCTCAGACCGCTTT-3' 5'-CATCATCGCTAATCACGACGC-3'	NM_013556.2	85	99.1
Pgk1	5'-CTCCGCTTTCATGTAGAGGAAG-3' 5'-GACATCTCCTAGTTTGGACAGTG-3'	NM_008828.3	117	109.1
Rpl13a	5'-CCCTCCACCCTATGACAAGAAAA-3' 5'-TAGGCTTCAGCCGAACAACC-3'	NM_009438.5	71	96.4
Tbp	5'-GGTATCTGCTGGCGGTTTGG-3' 5'-GAAATAGTGATGCTGGGCACTG-3'	NM_013684.3	73	99.7
Ywhaz	5'-TGTCACGGTGTGGACGC-3' 5'-ATGACGTCAAACGCTTCTGG-3'	NM_011740.3	119	100.8

3.2. Expression profiles based on raw Cq values

Descriptive statistics of Cq values for each B element and RG in hippocampus and cortex are depicted in Figs. A.1 and A.2 (Appendix A). In hippocampus, almost all genes and B elements show a similar expression pattern across age and genotype groups. In animals aged 24 months, however, higher levels of *B2m* can be discerned relative to animals aged 6–8 weeks and 6 months. Overall, the variation in Cq values represented by the interquartile range is larger in cortical tissue compared to hippocampal samples for all tested genes. Surprisingly, the expression profiles of the B elements in the cortex showed the highest variability.

3.3. Stability ranking of reference genes according to geNorm, NormFinder and BestKeeper

For both tissue types, the ranking of RGs was largely similar between the three algorithms. The ranking of all RGs and separate B elements, as well as their gene stability scores, are displayed in Table 2. In hippocampal tissue, B1 and B2 performed relatively well, with a top 5 ranking in the gene list generated by each algorithm (Fig. 1A–C). Furthermore, almost all genes included in the analysis proved to be acceptable RGs, indicated by the finding that all RGs had a geNorm M value < 0.50. Nevertheless, caution should be exercised when choosing *B2m* as RG in hippocampus, since this RG shows considerably higher stability indices compared to the other RGs in both NormFinder and BestKeeper algorithms. Furthermore, B elements and *B2m* were amongst the least favorably ranked genes in cortical tissue, crossing the geNorm M threshold value. NormFinder and BestKeeper algorithms both appear to confirm this finding, with distinctly higher stability indices for B elements as well as *B2m*. In addition, when both B1 and B2 were included, B1 had a higher ranking compared to B2 in hippocampus, while both SINEs were ranked as the two least stably expressed transcripts in cortex (Fig. 1D–F). As the BestKeeper algorithm is limited to 10 genes, *B2m* was excluded from the analysis since it was the least stably expressed transcript according to both geNorm and NormFinder.

3.4. Rank aggregation analysis

Although the ranking of all analyzed genes was fairly similar within tissue type, some genes performed differently when ranks were compared across algorithms. A final overall ranking including either B1 or B2, indicated that in hippocampus of the APP23 model, *Rpl13a* showed the most stable expression, followed by *Gapdh* and *Actb*. When a combination of both B elements was included, B1 was ranked as the fourth most stably expressed gene transcript, while B2 was ranked sixth. In cortex, *Actb*, *Tbp* and *Ywhaz*, showed the most stable transcript levels overall, whereas B1 and B2 were ranked last.

Since B1 and B2 had a very distinct stability in hippocampus compared to cortex, they were excluded from analysis when an overall ranking across tissues and across algorithms was performed, to obtain an indication of the most stable gene transcripts in experiments investigating gene expression levels in cortex and hippocampus. This rank aggregation returned *Actb* as the most stably expressed transcript, followed by *Gapdh* and *Ywhaz* (Table 3).

3.5. Number of reference genes to be included

The pairwise variation between normalization factors (NFs) incorporating n and n + 1 RGs, was lower than the proposed cut-off value of 0.15 for all n (Fig. 2). For hippocampal as well as cortical tissue, the pairwise variation between NFs containing two and three RGs was smaller than 0.15, indicating that the addition of a third gene was not required. However, the geNorm V values were consistently higher in cortex (Fig. 2B, Fig. A.3C, D in Appendix A) compared to hippocampus (Fig. 2A, Fig. A.3A, B in Appendix A), regardless of the number of candidate RGs.

3.6. Normalized expression of B elements and APP

Since the results of the geNorm V analysis indicated that two RGs should be included in the normalization panel, and as rank aggregation indicated the best RGs in either tissue, we normalized expression levels of B1 and B2 to the optimal NF in hippocampus (*Gapdh* and *Rpl13a*) and cortex (*Actb* and *Tbp*). Both SINEs are characterized by a stable

Table 2
Stability ranking of single B elements and RGs according to geNorm, NormFinder and BestKeeper in hippocampus and cortex. Gene ranks indicate the stability of gene expression, with 1 corresponding to the most stable gene, and 10 to the least stable. Abbreviations: *Actb*: beta-actin; *B2m*: beta-2-microglobulin; *Gapdh*: glyceraldehyde-3-phopshate dehydrogenase; geNorm M: average expression stability; *Gusb*: beta-glucuronidase; *Hprt*: hypoxanthine guanine phosphoribosyl transferase; *Pgk1*: phosphoglycerate kinase 1; RGs: reference genes; *Rpl13a*: ribosomal protein L13 A; *Tbp*: TATA-box binding protein; *Ywhaz*: tyrosine 3-monooxygenase/tryptophan 5-monooxygenase activation protein zeta.

Hippocampus						Cortex					
geNorm		NormFinder		BestKeeper		geNorm		NormFinder		BestKeeper	
Rank -Gene	geNorm M	Rank- Gene	Stability value	Rank- Gene	1-Correlation coefficient	Rank- Gene	geNorm M	Rank- Gene	Stability value	Rank- Gene	1-Correlation coefficient
B1 compared to RGs											
1-*Gapdh*	0.161	1-*Rpl13a*	0.173	1-*Rpl13a*	0.045	1-*Actb*	0.253	1-*Hprt*	0.087	1-*Actb*	0.079
2-*Actb*	0.168	2-*Hprt*	0.279	2-*Gapdh*	0.070	2-*Ywhaz*	0.261	2-*Tbp*	0.160	2-*Tbp*	0.083
3-*Ywhaz*	0.171	3-B1	0.296	3-*Actb*	0.072	3-*Tbp*	0.269	3-*Gapdh*	0.183	3-*Gapdh*	0.085
4-*Rpl13a*	0.201	4-*Gapdh*	0.297	4-*Pgk1*	0.074	4-*Gapdh*	0.305	4-*Ywhaz*	0.220	4-*Hprt*	0.111
5-B1	0.219	5-*Actb*	0.341	5-B1	0.084	5-*Hprt*	0.348	5-*Actb*	0.313	5-*Ywhaz*	0.113
6-*Pgk1*	0.232	6-*Gusb*	0.412	6-*Hprt*	0.131	6-*Pgk1*	0.388	6-*Pgk1*	0.346	6-*Pgk1*	0.115
7-*Tbp*	0.260	7-*Pgk1*	0.425	7-*Ywhaz*	0.147	7-*Rpl13a*	0.416	7-*Rpl13a*	0.440	7-*Rpl13a*	0.129
8-*Hprt*	0.288	8-*Tbp*	0.428	8-*Tbp*	0.165	8-*Gusb*	0.444	8-*Gusb*	0.452	8-*Gusb*	0.167
9-*Gusb*	0.324	9-*Ywhaz*	0.435	9-*Gusb*	0.182	9-*B2m*	0.517	9-*B2m*	0.628	9-B1	0.341
10-*B2m*	0.423	10-*B2m*	1.199	10-*B2m*	0.537	10-B1	0.653	10-B1	8.012	10-*B2m*	0.530
B2 compared to RGs											
1-*Gapdh*	0.161	1-*Rpl13a*	0.172	1-*Rpl13a*	0.042	1-*Actb*	0.253	1-*Hprt*	0.059	1-*Actb*	0.080
2-*Actb*	0.168	2-*Hprt*	0.281	2-*Gapdh*	0.065	2-*Ywhaz*	0.261	2-*Tbp*	0.148	2-*Tbp*	0.082
3-*Ywhaz*	0.171	3-*Gapdh*	0.288	3-*Actb*	0.069	3-*Tbp*	0.269	3-*Gapdh*	0.152	3-*Gapdh*	0.091
4-*Rpl13a*	0.201	4-*Actb*	0.337	4-*Pgk1*	0.073	4-*Gapdh*	0.305	4-*Ywhaz*	0.199	4-*Ywhaz*	0.110
5-*Pgk1*	0.220	5-B2	0.367	5-*Hprt*	0.131	5-*Hprt*	0.348	5-*Actb*	0.232	5-*Hprt*	0.129
6-B2	0.253	6-*Gusb*	0.418	6-*Ywhaz*	0.141	6-*Pgk1*	0.388	6-*Rpl13a*	0.312	6-*Pgk1*	0.142
7-*Tbp*	0.277	7-*Tbp*	0.423	7-*Tbp*	0.160	7-*Rpl13a*	0.416	7-*Gusb*	0.333	7-*Rpl13a*	0.151
8-*Hprt*	0.302	8-*Ywhaz*	0.425	8-B2	0.176	8-*Gusb*	0.444	8-*Pgk1*	0.450	8-*Gusb*	0.154
9-*Gusb*	0.337	9-*Pgk1*	0.429	9-*Gusb*	0.196	9-*B2m*	0.517	9-*B2m*	0.571	9-B2	0.474
10-*B2m*	0.435	10-*B2m*	1.203	10-*B2m*	0.550	10-B2	0.684	10-B2	3.308	10-*B2m*	0.515

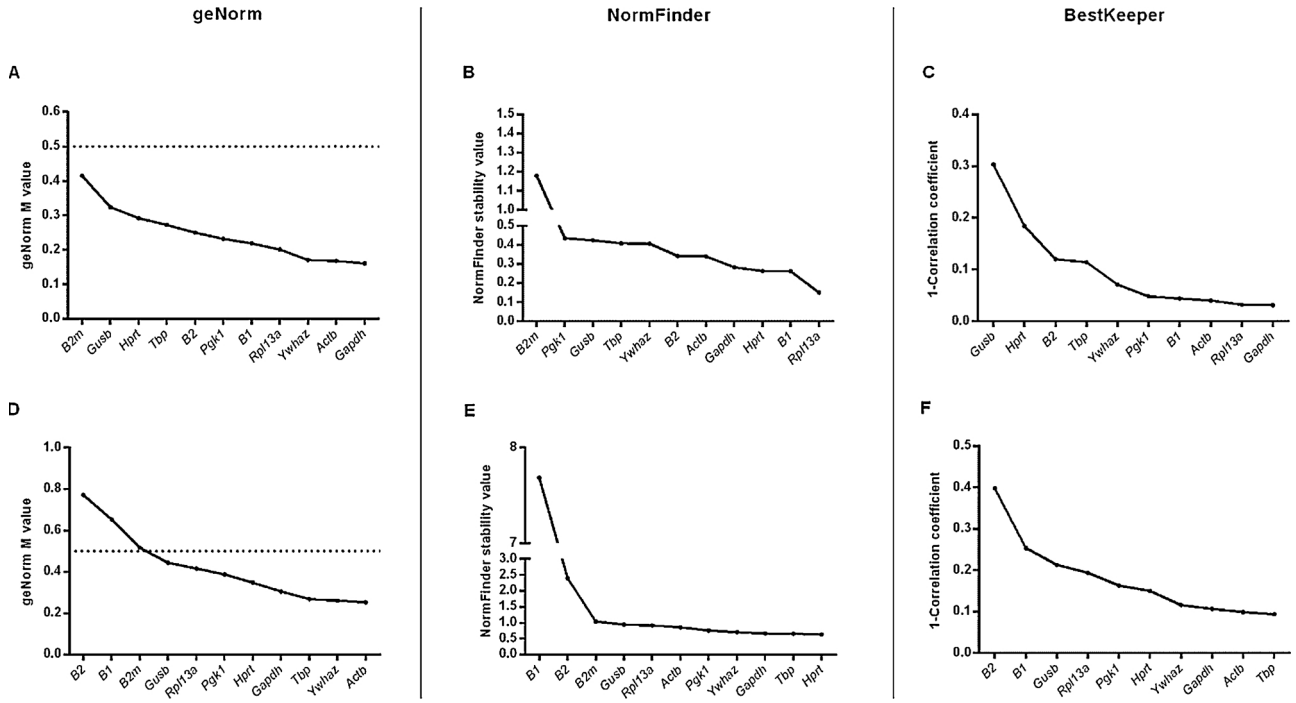

Fig. 1. Stability ranking of both B elements and RGs according to geNorm, NormFinder and BestKeeper. A, B, C depict findings in hippocampus, while D, E, F, illustrate results in cortex. The higher the stability value on the y-axis, the less stably the corresponding gene transcript is expressed. For geNorm analyses, the proposed geNorm M value cutoff of 0.50 is indicated by the dotted line. In case of BestKeeper analysis, *B2m* was not included as the algorithm is limited to a maximum of 10 genes and *B2m* was the least stably expressed RG as reported by geNorm and NormFinder. Abbreviations: *Actb*: beta-actin; *B2m*: beta-2-microglobulin; *Gapdh*: glyceraldehyde-3-phopshate dehydrogenase; geNorm M: average expression stability; *Gusb*: beta-glucuronidase; *Hprt*: hypoxanthine guanine phosphoribosyl transferase; *Pgk1*: phosphoglycerate kinase 1; RGs: reference genes; *Rpl13a*: ribosomal protein L13 A; *Tbp*: TATA-box binding protein; *Ywhaz*: tyrosine 3-monooxygenase/tryptophan 5-monooxygenase activation protein zeta.

Table 3
Final stability ranking of RGs after rank aggregation analysis implementing the cross-entropy Monte-Carlo algorithm with Spearman's footrule distance across algorithms and tissue types. Rank 1 corresponds to the most stably expressed RG, while rank 9 represents the least stable RG. Abbreviations: *Actb*: beta-actin; *B2m*: beta-2-microglobulin; *Gapdh*: glyceraldehyde-3-phopshate dehydrogenase; *Gusb*: beta-glucuronidase; *Hprt*: hypoxanthine guanine phosphoribosyl transferase; *Pgk1*: phosphoglycerate kinase 1; RG: reference gene; *Rpl13a*: ribosomal protein L13 A; *Tbp*: TATA-box binding protein; *Ywhaz*: tyrosine 3-monooxygenase/tryptophan 5-monooxygenase activation protein zeta.

Rank	RG
1	*Actb*
2	*Gapdh*
3	*Ywhaz*
4	*Hprt*
5	*Tbp*
6	*Rpl13a*
7	*Pgk1*
8	*Gusb*
9	*B2m*

expression in hippocampus across age and genotype, whereas in cortex, more variability across experimental conditions could be observed (Fig. 3). These observations were corroborated by the results of a two-way ANOVA, with non-significant effects of age [(F (2, 24) = 0.703; P = 0.505) and (F (2, 24) = 0.071; P = 0.932)] and genotype [(F (1, 24) = 0.163; P = 0.690) and (F (1, 24) = 0.158; P = 0.695)] on log-transformed NRQs of B1 and B2, respectively. Furthermore, no significant interaction effects between age and genotype were found for normalized expression of B1 (F (2, 24) = 0.104; P = 0.902) and B2 (F (2, 24) = 0.128; P = 0.880) in hippocampal tissue. Welch's ANOVA indicated a non-significant age effect on B1 levels in the cortex (Welch's F (2, 15.707) = 1.12; P = 0.352). An independent samples *t*-test indicated no significant effect of genotype on normalized B1 expression levels (T (28) = -1.182; P = 0.247). Similar results were found for B2, without significant effects of age (F (2, 24) = 1.389; P = 0.269) nor genotype (F (1, 24) = 0.009; P = 0.927), as well as a non-significant interaction term (F (2, 24) = 1.218; P = 0.313).

In addition, normalized expression of *APP* in hippocampus and cortex was also determined using previously determined optimal NF for each tissue (Fig. A.4, Appendix A). Transgenic APP23 animals were characterized by a (8.5 ± 0.9)-fold, (11.0 ± 3.0)-fold, and (10.2 ± 2.2)-fold overexpression of *APP* in hippocampal tissue of HET mice aged 6–8 weeks, 6 months and 24 months, respectively. Conversely, in cortical tissue, *APP* levels were expressed (2.1 ± 1.0)-fold in HET compared to WT animals aged 6–8 weeks, while a (3.8 ± 4.1)-fold and (19.4 ± 15.0)-fold overexpression were found in HET mice aged respectively 6 and 24 months. The results of a two-way ANOVA showed a significant effect of age (F (2, 24) = 9.162; P = 0.001) and genotype (F (1, 24) = 1849.160; P < 0.001) on normalized *APP* levels in hippocampus, while the difference between WT and HET animals was not significantly influenced by age (F (2, 24) = 2.173; P = 0.136). Regardless of genotype, differences in *APP* expression were found between the youngest age group (6–8 weeks) and the 6- (P = 0.001) and 24-month-old (P = 0.011) groups after Tukey's post-hoc tests. In contrast, NRQs of *APP* in WT versus HET animals were differently influenced by age in cortical tissue (F (2, 22) = 6.291; P = 0.007), despite a non-significant effect of age on *APP* levels (F (2, 22) = 1.676; P = 0.210) regardless of genotype. Genotype, however, did have a highly significant effect on *APP* expression in the cortex (F (2, 22) = 47.827; P < 0.001).

To investigate the use of B elements as a novel normalization approach, we also compared the *APP* expression profile across genotypes when normalized to B1, B2, and a combination of these B elements (Fig. 4). We found that the overexpression levels of *APP* in hippocampus were (9.8 ± 3.3)-fold, (10.3 ± 3.6)-fold, (10.1 ± 3.3)-fold, and (10.0 ± 2.7)-fold, when respective NFs containing B1, B2, B1 and B2, or *Rpl13a* and *Gapdh*, were implemented. In cortex, overexpression of *APP* in HET compared to WT animals was (6.1 ± 5.2)-fold, (6.9 ± 4.9)-fold, (6.5 ± 4.7)-fold, and (6.7 ± 8.1)-fold when B1, B2, a combination of these SINEs, or the optimal combination of *Actb* and *Tbp* were used as NF, respectively.

4. Discussion

4.1. Strengths and limitations

Our study comprised three equally sized age groups, from juvenile to old age, comprising WT and HET animals of the well characterized APP23 amyloidosis mouse model (Sturchler-Pierrat et al., 1997;

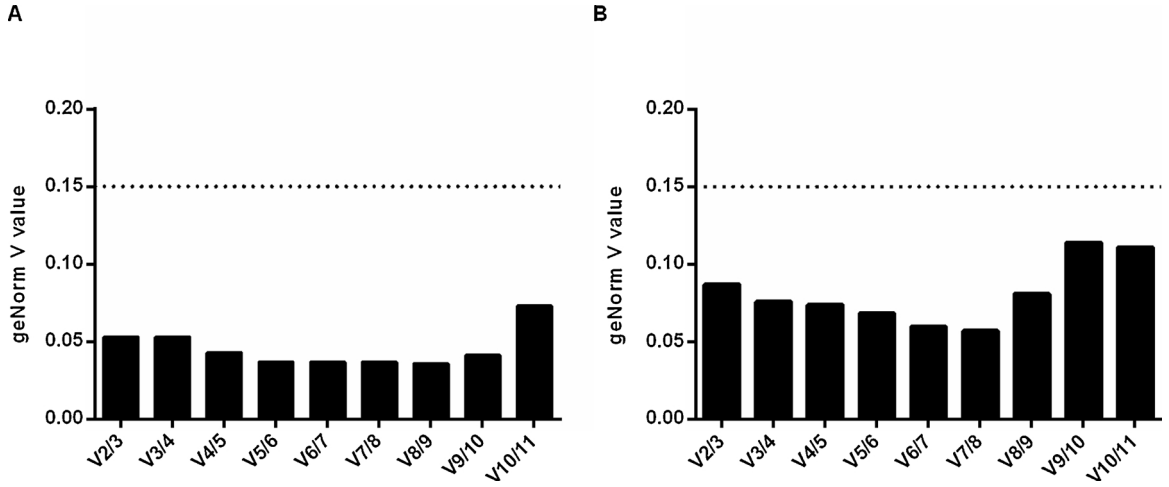

Fig. 2. Pairwise variation of NFs upon inclusion of an additional RG. geNorm analyses were performed in hippocampal tissue (A) and cortex (B), incorporating both B elements. The optimal number of RGs is indicated by the cutoff value of 0.15, below which the benefit of including an $(n+1)^{th}$ RG is limited. Abbreviations: NF: normalization factor; $V_{(n/n+1)}$: pairwise variation between normalization factors incorporating a consecutive number of reference genes; RG: reference gene.

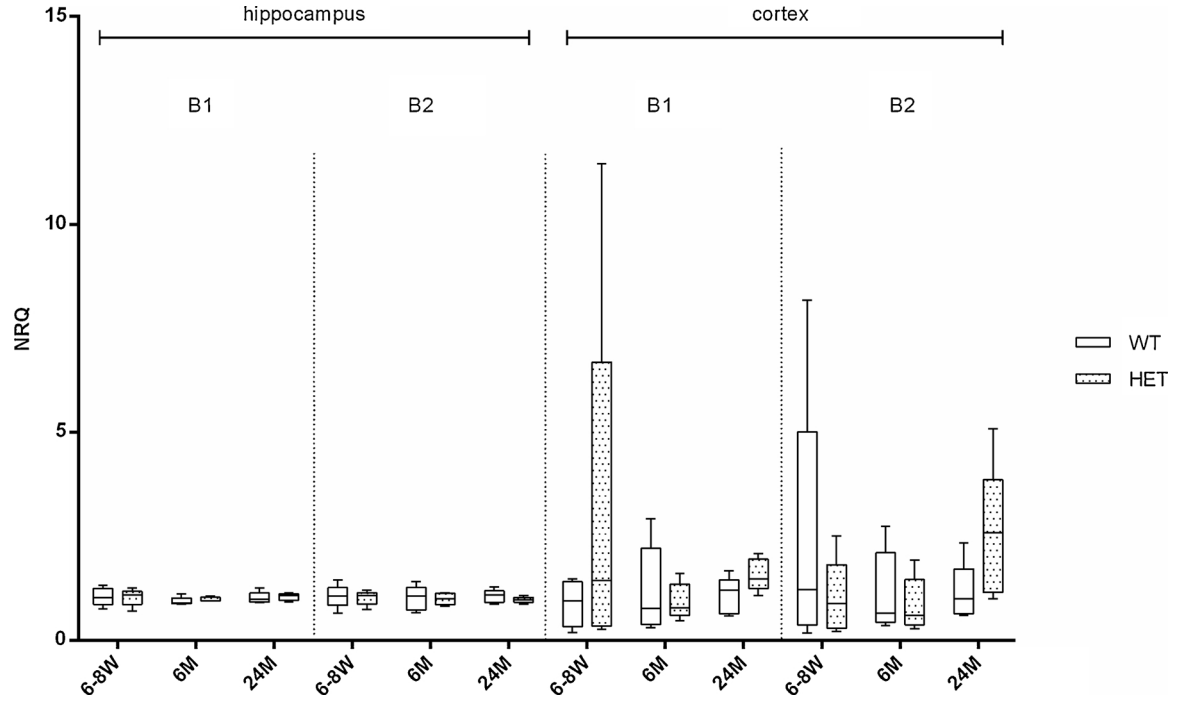

Fig. 3. Normalized expression levels of B1 and B2 in WT (n = 5) and HET (n = 5) mice by age group, to a normalization factor including *Gapdh* and *Rpl13a* in hippocampus, and *Actb* and *Tbp* in cortex. Data are represented as box and whisker plots with minimum and maximum values. Abbreviations: *Actb*: beta-actin; *Gapdh*: glyceraldehyde-3-phosphate dehydrogenase; HET: heterozygous; M: months; NRQ: normalized relative quantities; *Rpl13a*: ribosomal protein L13 A; SD: standard deviation; *Tbp*: TATA-box binding protein; W: weeks; WT: wild-type.

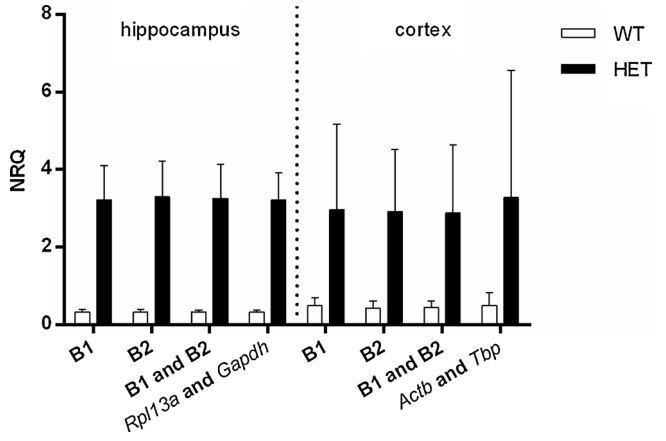

Fig. 4. *APP* overexpression levels in hippocampus and cortex. For hippocampus, NRQs of WT (n = 15) versus HET (n = 15) animals were obtained using four NFs, including either B1, B2, a combination of B1 and B2, and the optimal combination of *Rpl13a* and *Gapdh*. In case of cortical tissue, 13 WT and 15 HET animals were included for the analysis of APP levels normalized to B1, B2, a combination of these B elements, and the optimal NF comprising *Actb* and *Tbp*. Data are represented as mean ± SD. Abbreviations: *APP*: amyloid precursor protein; *Gapdh*: glyceraldehyde-3-phosphate dehydrogenase; HET: heterozygous; NFs: normalization factors; NRQ: normalized relative quantities; *Rpl13a*: ribosomal protein L13 A; SD: standard deviation; WT: wild-type.

Sturchler-Pierrat and Staufenbiel, 2000), thus introducing a considerable amount of biological variation and facilitating statistical analysis. In addition, nine commonly used RGs were analyzed in conjunction with two SINEs, using three independent gene ranking algorithms. Since those three algorithms indicated slightly different rankings, rank aggregation was performed to retrieve a final ranking of all RGs and B elements combined, adding further reliability to our study. Apart from gene stability analysis, we also conducted a normalization approach implementing B elements to investigate the expression of *APP*, which is known to be overexpressed in HET relative to WT mice. Despite the fact that no protein-level analyses were conducted, our study adds relevant information to the characterization of the APP23 model, unambiguously reporting *APP* transgene mRNA levels in transgenic versus WT mice.

A study aspect conceived as both a strength and a limitation, is that regional brain dissection was applied to collect brain samples. Although we have ample expertise in doing so and although this technique was performed with great precision, it gives rise to a larger amount of unwanted variability compared to other techniques such as laser capture microdissection. Moreover, the BestKeeper algorithm does not produce a gene ranking by itself. Other rankings, e.g. based on coefficient of variation and standard deviation, might give rise to alternative results. However, we believe that a gene ranking analysis should preferentially be based on the relation between genes or a measure taking into account distinct sources of variation, and, therefore, we chose to implement the correlation coefficient between each candidate RG and the BestKeeper Index.

4.2. Stability of B elements and commonly used reference genes in hippocampus and cortex

In both hippocampus and cortex, the results of the gene stability analysis were comparable between the three distinct algorithms, with B elements having stability values lower than the geNorm threshold value of 0.5 in hippocampus, while in cortex, their expression levels were less stable compared to the RGs, with stability values near or above the threshold. Two of the most implemented RGs in literature, *Actb* and *Gapdh* (Kozera and Rapacz, 2013; Suzuki et al., 2000), were in the top 5 of most stably expressed transcripts, with geNorm M values far below the threshold value, regardless of tissue type. Moreover, in the final rank merging all analysis methods and tissues, and including only commonly applied RGs, *Actb* and *Gapdh* were classified as the most stable candidate genes. These results do not entirely comply with previous reports on RG stability in the literature. A study investigating the

expression stability of six commonly reported RGs in brain regions of mice at postnatal day 7 and at 6 months of age, found that *Gapdh* was ranked sixth of all analyzed genes in the latter age group, with a geNorm M value of 13.396 (Boda et al., 2009). However, it should be noted that 6-month-old CD1 mice were first anesthetized by inhalation of isoflurane, followed by decapitation and brain collection, while our results were obtained in transgenic mice with a C57BL/6 J background and in the absence of potentially interfering anesthetics. Indeed, inhalation anesthesia with isoflurane has been reported to induce changes in mRNA, even after a short time span (Staib-Lasarzik et al., 2014). In contrast, another report, focusing on the stability of RGs in the developing mouse brain, indicated that *Actb* was the second most stably expressed RG in the male developing C57BL/6 mouse brain across time points ranging from embryonic day 11.5 until 15.5, with a GeoMean score of 2.73 (Cheung et al., 2017). As our study pinpointed aging and disease progression rather than development, and since we used a distinct method of euthanasia along with a different mouse model, it is difficult to compare our results with the findings of these previous studies.

4.3. Tissue-specific differences in stability of B elements

When B1 and B2 were normalized to the ideal normalization panel in hippocampus and cortex, both SINEs showed stable expression across hippocampal samples. Although still moderately stable, these SINEs were characterized by a lesser stability in cortex compared to hippocampus. Surprisingly, no significant effects of age or genotype were found in normalized B1 nor B2 levels in the cortex, while their mean values vary considerably (Fig. 3). Possibly, the variation in normalized levels of the B elements was too high to detect a statistically significant difference. Although the macroscopic dissection method used for this work is not as accurate as laser capture microdissection, it is unlikely this influenced our findings. Despite the fact that all samples were visually checked for the presence of pieces of white matter, we cannot exclude the possibility that some traces were still present in the collected samples, thereby minimally altering the relative amount of cortex tissue. However, applying laser capture microdissection, would have made the tissue collection process more labor-intensive and time-consuming. Secondly, epigenetic changes such as DNA methylation or histone modification are hallmarks of genomic instability (Li and Zhang, 2014) and might underlie the disparity with regard to the stability of B elements in hippocampus versus cortex. As such, B1 elements were found to be methylated in somatic (Ichiyanagi, 2013) and embryonic cells (Papin et al., 2017), with a higher degree of methylation and subsequent transcriptional repression, compared to B2 (Papin et al., 2017).

Besides B elements, human Alu sequences are also known methylation targets (Jang et al., 2017; Kochanek et al., 1993; Luo et al., 2014). In addition, these SINEs were previously shown to exhibit age- and tissue-specific differential methylation (Ianov et al., 2017; Maegawa et al., 2010; Singhal et al., 1987; Thompson et al., 2010). One study even showed that methylation differences between brain areas were more apparent than differences in methylation profile with respect to age, gender, postmortem delay, race, diagnosis, or cause of death (Ladd-Acosta et al., 2007).

Since we did not generate proof of the nature, nor the direction of epigenetic changes, we can only speculate that a tissue-specific differential degree of epigenetic signaling across age groups and, possibly, genotypes, underlies the differences in the stability of B elements in cortex versus hippocampus. However, to the best of our knowledge, no reports exist of distinct age-or genotype-related epigenetic regulation of SINE expression in brain areas of the APP23 model. Since the first amyloid beta (Aβ)-plaques appear in the frontal cortex of HET APP23 mice aged 6 months (Sturchler-Pierrat and Staufenbiel, 2000), preceded by an increase in soluble Aβ oligomers from the age of 6–8 weeks onwards (Janssen et al., 2016), one could hypothesize that this brain region displays early epigenetic changes as a consequence of initial Aβ exposure, as was previously suggested in female mice of the 5xFAD model (Griñán-Ferré et al., 2016; Oakley et al., 2006) and in murine cerebral endothelial cells exposed to synthetic $A\beta_{1\text{-}40}$ peptides (Chen et al., 2009). However, one would also expect similar alterations in hippocampal samples of older age groups of the APP23 model, as amyloid plaques are present in virtually all brain regions in HET APP23 mice aged 24 months (Sturchler-Pierrat and Staufenbiel, 2000). Thus, it remains unclear why B elements are less stably expressed in cortex compared to hippocampus.

4.4. APP overexpression to validate the use of B elements as a novel normalization approach

Previously, the transgene in APP23 HET animals was reported to be sevenfold overexpressed relative to endogenous *App* mRNA, as determined by semi-quantitative PCR and confirmed by western blot experiments (Sturchler-Pierrat et al., 1997; Sturchler-Pierrat and Staufenbiel, 2000). However, it is unclear if these expression levels were determined across several ages or in a single age group. The use of a semi-quantitative technique, along with the number of tissue samples included in these analyses, further hamper a straightforward comparison of our *APP* overexpression data with these initially reported results. However, regardless of age, *APP* was at least twofold overexpressed in HET relative to WT animals in the cortex of the youngest age group, while an increasing trend was observed in the older groups (Fig. A.4, Appendix A). Conversely, tissue samples derived from hippocampus showed a relatively constant expression of *APP* in all age groups. Thus, as suggested in the original paper describing the APP23 model, crossing a certain threshold expression of *APP* bearing human disease-associated mutations, might represent an initial incentive for neuropathology (Sturchler-Pierrat et al., 1997). In addition, a specific threshold of two- to threefold *APP* overexpression was previously proposed for successful reproduction of pathological AD-like features (Guénette and Tanzi, 1999). In the youngest age group of this study, *APP* is also overexpressed in HET versus WT animals, although no plaque-related neuropathology is present at this age. However, as stated previously, high levels of soluble Aβ oligomers were found at this early stage (Janssen et al., 2016) as a possible result of initial *APP* overexpression. Lastly, when hippocampal *APP* levels were not only normalized to the ideal panel of RGs, but also to B1, B2, or a combination of both (Fig. 4), the overexpression of human *APP* was almost identical across all normalization strategies, indicating that these SINEs can indeed be adopted as a novel normalization approach in hippocampus. In cortex, the results of Fig. 4 appear to indicate that B1, B2 and a combination of these SINEs are superior to the previously determined optimal NF consisting of *Actb* and *Tbp*. However, one should bear in mind that this figure depicts normalized *APP* levels and that the large standard deviation of *APP* NRQs, when the optimal NF was used for normalization purposes, might just reflect a large biological variation of *APP* levels in the cortex of HET mice. In this aspect, B elements as NF in cortex might fail to indicate the actual results, leading researchers to draw incorrect conclusions. Conversely, a recent paper showed that 11 expressed repeat elements in mice, other than B1 and B2 (amongst others lower in copy number), were superior to commonly used RGs in the literature with respect to normalization purposes in a wide range of experimental setups (Renard et al., 2018). Thus, as contemporary research is providing growing evidence concerning the applicability of repeat elements with respect to normalization of mRNA expression levels in various conditions (Marullo et al., 2010; Renard et al., 2018; Rihani et al., 2013; Vanhauwaert et al., 2014), they might become increasingly popular as reference targets.

In conclusion, this study emphasizes the importance of validating RGs in distinct tissue types for optimal normalization results. The expression levels of B elements and *APP* varied to a much larger extent in cortex compared to hippocampus, which might be due to epigenetic

alterations. In addition, we provide first evidence for the use of mouse B elements as an alternative normalization approach in hippocampus, but not cortex, of the APP23 amyloidosis mouse model.

Declarations of interest

None.

Author contributions

Conception and design of the study: K.V.C., R.C., C.P.S., J.V., D.V.D., J.J.; Acquisition and analysis of data: J.J., Interpretation of data: D.V.D., J.J., Article draft: J.J., Revision: R.C., D.V.D., P.P.D.D., C.P.S., J.V.

Acknowledgements

This work was supported by the IWT/SBO research grant (No. 140028) and the SAO-FRA grant awarded to dr. D. Van Dam (No. 2017/0025), Research Foundation Flanders, the agreement between Institute Born-Bunge and the University of Antwerp, the Medical Research Foundation Antwerp, the Thomas Riellaerts research fund, and Neurosearch Antwerp. These funding sources had no influence on this work.

Appendix A. Supplementary data

Supplementary material related to this article can be found, in the online version, at doi:https://doi.org/10.1016/j.jneumeth.2019.03.005.

References

Andersen, C.L., Jensen, J.L., ørntoft, T.F., 2004. Normalization of real-time quantitative reverse transcription-PCR data: a model-based variance estimation approach to identify genes suited for normalization, applied to bladder and colon cancer data sets. Cancer Res. 64, 5245–5250. https://doi.org/10.1158/0008-5472.CAN-04-0496.

Boda, E., Pini, A., Hoxha, E., Parolisi, R., Tempia, F., 2009. Selection of reference genes for quantitative real-time RT-PCR studies in mouse brain. J. Mol. Neurosci. 37, 238–253. https://doi.org/10.1007/s12031-008-9128-9.

Bovine Genome Sequencing Analysis Consortium, Elsik, C.G., Tellam, R.L., Worley, K.C., Gibbs, R.A., Muzny, D.M., et al., 2009. The genome sequence of taurine cattle: a window to ruminant biology and evolution. Science 324, 522–528. https://doi.org/10.1126/science.1169588.

Brosius, J., 1999. RNAs from all categories generate retrosequences that may be exapted as novel genes or regulatory elements. Gene 238, 115–134. https://doi.org/10.1016/S0378-1119(99)00227-9.

Bustin, S.A., 2000. Absolute quantification of mRNA using real-time reverse transcription polymerase chain reaction assays. J. Mol. Endocrinol. 25, 169–193. https://doi.org/10.1677/jme.0.0250169.

Bustin, S.A., Benes, V., Nolan, T., Pfaffl, M.W., 2005. Quantitative real-time RT-PCR–a perspective. J. Mol. Endocrinol. 34, 597–601. https://doi.org/10.1677/jme.1.01755.

Bustin, S.A., Benes, V., Garson, J.A., Hellemans, J., Huggett, J., Kubista, M., et al., 2009. The MIQE guidelines: minimum information for publication of quantitative real-time PCR experiments. Clin. Chem. 55, 611–622. https://doi.org/10.1373/clinchem.2008.112797.

Bustin, S.A., Benes, V., Garson, J., Hellemans, J., Huggett, J., Kubista, M., et al., 2013. The need for transparency and good practices in the qPCR literature. Nat. Methods 10, 1063–1067. https://doi.org/10.1038/nmeth.2697.

Chapman, J.R., Waldenström, J., 2015. With reference to reference genes: a systematic review of endogenous controls in gene expression studies. PLoS One 10, e0141853. https://doi.org/10.1371/journal.pone.0141853.

Chen, K.L., Wang, S.S., Yang, Y.Y., Yuan, R.Y., Chen, R.M., Hu, C.J., 2009. The epigenetic effects of amyloid-beta(1-40) on global DNA and neprilysin genes in murine cerebral endothelial cells. Biochem. Biophys. Res. Commun. 378, 57–61. https://doi.org/10.1016/j.bbrc.2008.10.173.

Cheung, T.T., Weston, M.K., Wilson, M.J., 2017. Selection and evaluation of reference genes for analysis of mouse (Mus musculus) sex-dimorphic brain development. PeerJ 5, e2909. https://doi.org/10.7717/peerj.2909.

Crans, R.A.J., Janssens, J., Daelemans, S., Wouters, E., Raedt, R., Van Dam, D., et al., 2019. The validation of Short Interspersed Nuclear Elements (SINEs) as a RT-qPCR normalization strategy in a rodent model for temporal lobe epilepsy. PLoS One 14, e0210567. https://doi.org/10.1371/journal.pone.0210567.

Daniels, G.R., Deininger, P.L., 1985. Repeat sequence families derived from mammalian tRNA genes. Nature 317, 819–822. https://doi.org/10.1038/317819a0.

de Jonge, H.J., Fehrmann, R.S., de Bont, E.S., Hofstra, R.M., Gerbens, F., Kamps, W.A., et al., 2007. Evidence based selection of housekeeping genes. PLoS One 2, e898. https://doi.org/10.1371/journal.pone.0000898.

De Spiegelaere, W., Dern-Wieloch, J., Weigel, R., Schumacher, V., Schorle, H., Nettersheim, D., et al., 2015. Reference gene validation for RT-qPCR, a note on different available software packages. PLoS One 10, e0122515. https://doi.org/10.1371/journal.pone.0122515.

Deininger, P., 2011. Alu elements: know the SINEs. Genome Biol. 12, 236. https://doi.org/10.1186/gb-2011-12-12-236.

Eissa, N., Hussein, H., Wang, H., Rabbi, M.F., Bernstein, C.N., Ghia, J.E., 2016. Stability of reference genes for messenger RNA quantification by real-time PCR in mouse dextran sodium sulfate experimental colitis. PLoS One 11, e0156289. https://doi.org/10.1371/journal.pone.0156289.

Elbarbary, R.A., Lucas, B.A., Maquat, L.E., 2016. Retrotransposons as regulators of gene expression. Science 351, aac7247. https://doi.org/10.1126/science.aac7247.

Fronhoffs, S., Totzke, G., Stier, S., Wernert, N., Rothe, M., Brüning, T., et al., 2002. A method for the rapid construction of cRNA standard curves in quantitative real-time reverse transcription polymerase chain reaction. Mol. Cell. Probes 16, 99–110. https://doi.org/10.1006/mcpr.2002.0405.

Griñán-Ferré, C., Sarroca, S., Ivanova, A., Puigoriol-Illamola, D., Aguado, F., Camins, A., et al., 2016. Epigenetic mechanisms underlying cognitive impairment and Alzheimer disease hallmarks in 5XFAD mice. Aging 8, 664–684. https://doi.org/10.18632/aging.100906.

Guénette, S.Y., Tanzi, R.E., 1999. Progress toward valid transgenic mouse models for Alzheimer's disease. Neurobiol. Aging 20, 201–211. https://doi.org/10.1016/s0197-4580(99)00042-1.

Guénin, S., Mauriat, M., Pelloux, J., Van Wuytswinkel, O., Bellini, C., Gutierrez, L., 2009. Normalization of qRT-PCR data: the necessity of adopting a systematic, experimental conditions-specific, validation of references. J. Exp. Bot. 60, 487–493. https://doi.org/10.1093/jxb/ern305.

Hellemans, J., Mortier, G., De Paepe, A., Speleman, F., Vandesompele, J., 2007. qBase relative quantification framework and software for management and automated analysis of real-time quantitative PCR data. Genome Biol. 8, R19. https://doi.org/10.1186/gb-2007-8-2-r19.

Houck, C.M., Rinehart, F.P., Schmid, C.W., 1979. A ubiquitous family of repeated DNA sequences in the human genome. J. Mol. Biol. 132, 289–306. https://doi.org/10.1016/0022-2836(79)90261-4.

Ianov, L., Riva, A., Kumar, A., Foster, T.C., 2017. DNA methylation of synaptic genes in the prefrontal cortex is associated with aging and age-related cognitive impairment. Front. Aging Neurosci. 9, 249. https://doi.org/10.3389/fnagi.2017.00249.

Ichiyanagi, K., 2013. Epigenetic regulation of transcription and possible functions of mammalian short interspersed elements. SINEs. Genes Genet. Syst. 88, 19–29. https://doi.org/10.1266/ggs.88.19.

Jang, H.S., Shin, W.J., Lee, J.E., Do, J.T., 2017. CpG and non-CpG methylation in epigenetic gene regulation and brain function. Genes 8, 148. https://doi.org/10.3390/genes8060148.

Janssen, L., Keppens, C., De Deyn, P.P., Van Dam, D., 2016. Late age increase in soluble amyloid-beta levels in the APP23 mouse model despite steady-state levels of amyloid-beta-producing proteins. Biochim. Biophys. Acta 1862, 105–112. https://doi.org/10.1016/j.bbadis.2015.10.027.

Kochanek, S., Renz, D., Doerfler, W., 1993. DNA methylation in the Alu sequences of diploid and haploid primary human cells. EMBO J. 12, 1141–1151. https://doi.org/10.1002/j.1460-2075.1993.tb05755.x.

Kozera, B., Rapacz, M., 2013. Reference genes in real-time PCR. J. Appl. Genet. 54, 391–406. https://doi.org/10.1007/s13353-013-0173-x.

Kramerov, D.A., Grigoryan, A.A., Ryskov, A.P., Georgiev, G.P., 1979. Long double-stranded sequences (dsRNA-B) of nuclear pre-mRNA consist of a few highly abundant classes of sequences: evidence from DNA cloning experiments. Nucleic Acids Res. 6, 697–713. https://doi.org/10.1093/nar/6.2.697.

Krayev, A.S., Kramerov, D.A., Skryabin, K.G., Ryskov, A.P., Bayev, A.A., Georgiev, G.P., 1980. The nucleotide sequence of the ubiquitous repetitive DNA sequence B1 complementary to the most abundant class of mouse fold-back RNA. Nucleic Acids Res. 8, 1201–1215. https://doi.org/10.1093/nar/8.6.1201.

Krayev, A.S., Markusheva, T.V., Kramerov, D.A., Ryskov, A.P., Skryabin, K.G., Bayev, A.A., et al., 1982. Ubiquitous transposon-like repeats B1 and B2 of the mouse genome: B2 sequencing. Nucleic Acids Res. 10, 7461–7475. https://doi.org/10.1093/nar/10.23.7461.

Labuda, D., Sinnett, D., Richer, C., Deragon, J.M., Striker, G., 1991. Evolution of mouse B1 repeats: 7SL RNA folding pattern conserved. J. Mol. Evol. 32, 405–414. https://doi.org/10.1007/bf02101280.

Ladd-Acosta, C., Pevsner, J., Sabunciyan, S., Yolken, R.H., Webster, M.J., Dinkins, T., et al., 2007. DNA methylation signatures within the human brain. Am. J. Hum. Genet. 81, 1304–1315. https://doi.org/10.1086/524110.

Lander, E.S., Linton, L.M., Birren, B., Nusbaum, C., Zody, M.C., Baldwin, J., et al., 2001. Initial sequencing and analysis of the human genome. Nature 409, 860–921. https://doi.org/10.1038/35057062.

Lev-Maor, G., Sorek, R., Shomron, N., Ast, G., 2003. The birth of an alternatively spliced exon: 3' splice-site selection in Alu exons. Science 300, 1288–1291. https://doi.org/10.1126/science.1082588.

Li, E., Zhang, Y., 2014. DNA methylation in mammals. Cold Spring Harb. Perspect. Biol. 6, a019133. https://doi.org/10.1101/cshperspect.a019133.

Lindblad-Toh, K., Wade, C.M., Mikkelsen, T.S., Karlsson, E.K., Jaffe, D.B., Kamal, M., et al., 2005. Genome sequence, comparative analysis and haplotype structure of the domestic dog. Nature 438, 803–819. https://doi.org/10.1038/nature04338.

Livak, K.J., Schmittgen, T.D., 2001. Analysis of relative gene expression data using real-time quantitative PCR and the 2(-Delta Delta C(T)) method. Methods 25, 402–408.

https://doi.org/10.1006/meth.2001.1262.
Lucas, B.A., Lavi, E., Shiue, L., Cho, H., Katzman, S., Miyoshi, K., et al., 2018. Evidence for convergent evolution of SINE-directed Staufen-mediated mRNA decay. Proc. Natl. Acad. Sci. 115, 968–973. https://doi.org/10.1073/pnas.1715531115.
Maegawa, S., Hinkal, G., Kim, H.S., Shen, L., Zhang, L., Zhang, J., et al., 2010. Widespread and tissue specific age-related DNA methylation changes in mice. Genome Res. 20, 332–340. https://doi.org/10.1101/gr.096826.109.
Marullo, M., Zuccato, C., Mariotti, C., Lahiri, N., Tabrizi, S.J., Di Donato, S., et al., 2010. Expressed Alu repeats as a novel, reliable tool for normalization of real-time quantitative RT-PCR data. Genome Biol. 11, R9. https://doi.org/10.1186/gb-2010-11-1-r9.
Mikkelsen, T.S., Wakefield, M.J., Aken, B., Amemiya, C.T., Chang, J.L., Duke, S., et al., 2007. Genome of the marsupial Monodelphis domestica reveals innovation in non-coding sequences. Nature 447, 167–177. https://doi.org/10.1038/nature05805.
Mouse Genome Sequencing Consortium, Waterston, R.H., Lindblad-Toh, K., Birney, E., Rogers, J., Abril, J.F., et al., 2002. Initial sequencing and comparative analysis of the mouse genome. Nature 420, 520–562. https://doi.org/10.1038/nature01262.
Oakley, H., Cole, S.L., Logan, S., Maus, E., Shao, P., Craft, J., et al., 2006. Intraneuronal beta-amyloid aggregates, neurodegeneration, and neuron loss in transgenic mice with five familial Alzheimer's disease mutations: potential factors in amyloid plaque formation. J. Neurosci. 26, 10129–10140. https://doi.org/10.1523/JNEUROSCI.1202-06.2006.
Papin, C., Ibrahim, A., Gras, S.L., Velt, A., Stoll, I., Jost, B., et al., 2017. Combinatorial DNA methylation codes at repetitive elements. Genome Res. 27, 934–946. https://doi.org/10.1101/gr.213983.116.
Pfaffl, M.W., Hageleit, M., 2001. Validities of mRNA quantification using recombinant RNA and recombinant DNA external calibration curves in real-time RT-PCR. Biotechnol. Lett. 23, 275–282. https://doi.org/10.1023/A:1005658330108.
Pihur, V., Datta, S., Datta, S., 2009. RankAggreg, an R package for weighted rank aggregation. BMC Bioinformatics 10, 62. https://doi.org/10.1186/1471-2105-10-62.
Renard, M., Vanhauwaert, S., Vanhomwegen, M., Rihani, A., Vandamme, N., Goossens, S., et al., 2018. Expressed repetitive elements are broadly applicable reference targets for normalization of reverse transcription-qPCR data in mice. Sci. Rep. 8, 7642. https://doi.org/10.1038/s41598-018-25389-6.
Rihani, A., Van Maerken, T., Pattyn, F., Van Peer, G., Beckers, A., De Brouwer, S., et al., 2013. Effective Alu repeat based RT-Qpcr normalization in cancer cell perturbation experiments. PLoS One 8, e71776. https://doi.org/10.1371/journal.pone.0071776.
Rydbirk, R., Folke, J., Winge, K., Aznar, S., Pakkenberg, B., Brudek, T., 2016. Assessment of brain reference genes for RT-qPCR studies in neurodegenerative diseases. Sci. Rep. 6, 37116. https://doi.org/10.1038/srep37116.
Ryskov, A.P., Farashyan, V.R., Georgiev, G.P., 1972. Ribonuclease-stable base sequences specific exclusively for giant dRNA. Biochim. Biophys. Acta 262, 568–572. https://doi.org/10.1016/0005-2787(72)90502-3.
Ryskov, A.P., Saunders, G.F., Farashyan, V.R., Georgiev, G.P., 1973. Double-helical regions in nuclear precursor of mRNA (pre-mRNA). Biochim. Biophys. Acta 312, 152–164. https://doi.org/10.1016/0005-2787(73)90060-9.
Sakamoto, K., Okada, N., 1985. Rodent type 2 Alu family, rat identifier sequence, rabbit C family, and bovine or goat 73-bp repeat may have evolved from tRNA genes. J. Mol. Evol. 22, 134–140. https://doi.org/10.1007/bf02101691.
Sasaki, T., Nishihara, H., Hirakawa, M., Fujimura, K., Tanaka, M., Kokubo, N., et al., 2008. Possible involvement of SINEs in mammalian-specific brain formation. Proc. Natl. Acad. Sci. U. S. A. 105, 4220–4225. https://doi.org/10.1073/pnas.0709398105.
Singer, M.F., 1982. SINEs and LINEs: highly repeated short and long interspersed sequences in mammalian genomes. Cell 28, 433–434. https://doi.org/10.1016/0092-8674(82)90194-5.
Singhal, R.P., Mays-Hoopes, L.L., Eichhorn, G.L., 1987. DNA methylation in aging of mice. Mech. Ageing Dev. 41, 199–210. https://doi.org/10.1016/0047-6374(87)90040-6.
Sorek, R., Ast, G., Graur, D., 2002. Alu-containing exons are alternatively spliced. Genome Res. 12, 1060–1067. https://doi.org/10.1101/gr.229302.
Staib-Lasarzik, I., Kriege, O., Timaru-Kast, R., Pieter, D., Werner, C., Engelhard, K., et al., 2014. Anesthesia for euthanasia influences mRNA expression in healthy mice and after traumatic brain injury. J. Neurotrauma 31, 1664–1671. https://doi.org/10.1089/neu.2013.3243.
Sturchler-Pierrat, C., Staufenbiel, M., 2000. Pathogenic mechanisms of Alzheimer's disease analyzed in the APP23 transgenic mouse model. Ann. NY Acad. Sci. 920, 134–139. https://doi.org/10.1111/j.1749-6632.2000.tb06915.x.
Sturchler-Pierrat, C., Abramowski, D., Duke, M., Wiederhold, K.H., Mistl, C., Rothacher, S., et al., 1997. Two amyloid precursor protein transgenic mouse models with Alzheimer disease-like pathology. Proc. Natl. Acad. Sci. U. S. A. 94, 13287–13292. https://doi.org/10.1073/pnas.94.24.13287.
Suzuki, T., Higgins, P.J., Crawford, D.R., 2000. Control selection for RNA quantitation. Biotechniques 29, 332–337. https://doi.org/10.2144/00292rv02.
Svingen, T., Letting, H., Hadrup, N., Hass, U., Vinggaard, A.M., 2015. Selection of reference genes for quantitative RT-PCR (RT-qPCR) analysis of rat tissues under physiological and toxicological conditions. PeerJ 3, e855. https://doi.org/10.7717/peerj.855.
Thompson, R.F., Atzmon, G., Gheorghe, C., Liang, H.Q., Lowes, C., Greally, J.M., et al., 2010. Tissue-specific dysregulation of DNA methylation in aging. Aging Cell 9, 506–518. https://doi.org/10.1111/j.1474-9726.2010.00577.x.
Tomilin, N.V., 1999. Control of genes by mammalian retroposons. Int. Rev. Cytol. 186, 1–48. https://doi.org/10.1016/s0074-7696(08)61050-5.
Tommasi, S., Zheng, A., Weninger, A., Bates, S.E., Li, X.A., Wu, X., et al., 2013. Mammalian cells acquire epigenetic hallmarks of human cancer during immortalization. Nucleic Acids Res. 41, 182–195. https://doi.org/10.1093/nar/gks1051.
Tsirigos, A., Rigoutsos, I., 2009. Alu and b1 repeats have been selectively retained in the upstream and intronic regions of genes of specific functional classes. PLoS Comput. Biol. 5, e1000610. https://doi.org/10.1371/journal.pcbi.1000610.
Ullu, E., Tschudi, C., 1984. Alu sequences are processed 7SL RNA genes. Nature 312, 171–172. https://doi.org/10.1038/312171a0.
Van Dam, D., De Deyn, P.P., 2011. APP-based transgenic models: the APP23 model. In: De Deyn, P.P., Van Dam, D. (Eds.), Animal Models of Dementia. Humana Press, New York, pp. 399–414. https://doi.org/10.1007/978-1-60761-898-0_20.
Van Dam, D., Vloeberghs, E., Abramowski, D., Staufenbiel, M., De Deyn, P.P., 2005. APP23 mice as a model of Alzheimer's disease: an example of a transgenic approach to modeling a CNS disorder. CNS Spectr. 10, 207–222. https://doi.org/10.1017/s1092852900010051.
Vandesompele, J., De Preter, K., Pattyn, F., Poppe, B., Van Roy, N., De Paepe, A., et al., 2002. Accurate normalization of real-time quantitative RT-PCR data by geometric averaging of multiple internal control genes. Genome Biol. 3 RESEARCH0034.
Vanhauwaert, S., Van Peer, G., Rihani, A., Janssens, E., Rondou, P., Lefever, S., et al., 2014. Expressed repeat elements improve RT-qPCR normalization across a wide range of zebrafish gene expression studies. PLoS One 9, e109091. https://doi.org/10.1371/journal.pone.0109091.
Veniaminova, N.A., Vassetzky, N.S., Kramerov, D.A., 2007. B1 SINEs in different rodent families. Genomics 89, 678–686. https://doi.org/10.1016/j.ygeno.2007.02.007.
Vossaert, L., O'Leary, T., Van Neste, C., Heindryckx, B., Vandesompele, J., De Sutter, P., et al., 2013. Reference loci for RT-qPCR analysis of differentiating human embryonic stem cells. BMC Mol. Biol. 14, 21. https://doi.org/10.1186/1471-2199-14-21.
Weiner, A.M., 1980. An abundant cytoplasmic 7S RNA is complementary to the dominant interspersed middle repetitive DNA sequence family in the human genome. Cell 22, 209–218. https://doi.org/10.1016/0092-8674(80)90169-5.
Williams, W.P., Tamburic, L., Astell, C.R., 2004. Increased levels of B1 and B2 SINE transcripts in mouse fibroblast cells due to minute virus of mice infection. Virology 327, 233–241. https://doi.org/10.1016/j.virol.2004.06.040.